

Plasmonic-enhanced performance for polymer solar cells prepared with inverted structures

Chuan-Sheng Kao, Fang-Chung Chen, Ching-Wen Liao, Michael H. Huang, and Chain-Shu Hsu

Citation: [Applied Physics Letters](#) **101**, 193902 (2012); doi: 10.1063/1.4766736

View online: <http://dx.doi.org/10.1063/1.4766736>

View Table of Contents: <http://scitation.aip.org/content/aip/journal/apl/101/19?ver=pdfcov>

Published by the [AIP Publishing](#)

Articles you may be interested in

[Enhancement of short-circuit current density in polymer bulk heterojunction solar cells comprising plasmonic silver nanowires](#)

Appl. Phys. Lett. **104**, 123302 (2014); 10.1063/1.4869760

[Performance improvement of inverted polymer solar cells by doping Au nanoparticles into TiO₂ cathode buffer layer](#)

Appl. Phys. Lett. **103**, 233303 (2013); 10.1063/1.4840319

[Efficiency enhancement of polymer solar cells by localized surface plasmon of Au nanoparticles](#)

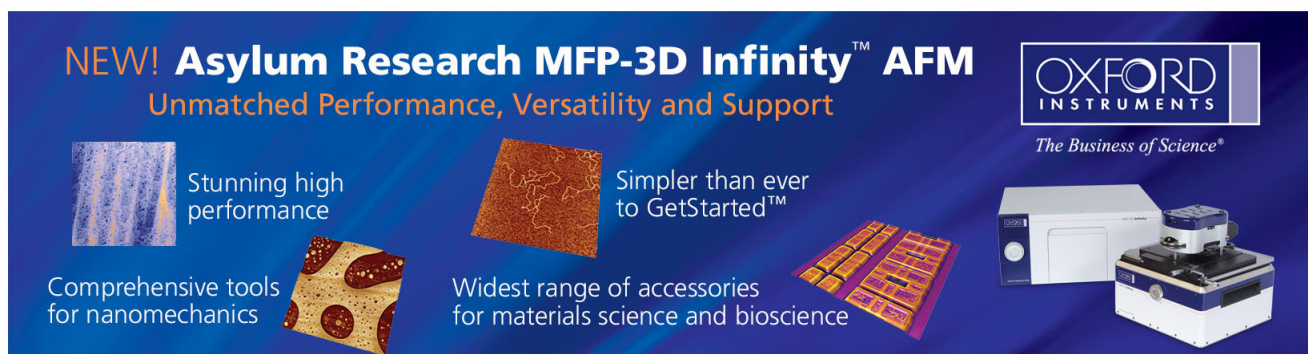
J. Appl. Phys. **114**, 163102 (2013); 10.1063/1.4827181

[The role of Ag nanoparticles in inverted polymer solar cells: Surface plasmon resonance and backscattering centers](#)

Appl. Phys. Lett. **102**, 123301 (2013); 10.1063/1.4798553

[Effect of textured electrodes with light-trapping on performance of polymer solar cells](#)

J. Appl. Phys. **111**, 104516 (2012); 10.1063/1.4720083

The advertisement features a dark blue background with white and orange text. At the top left, it reads 'NEW! Asylum Research MFP-3D Infinity™ AFM' in large white letters, followed by 'Unmatched Performance, Versatility and Support' in orange. On the right, the Oxford Instruments logo is shown with the tagline 'The Business of Science®'. Below the text are four images: a blue textured surface, a brown textured surface, a grid of colorful squares, and the MFP-3D Infinity AFM instrument. Text descriptions are placed around these images: 'Stunning high performance' next to the blue surface, 'Simpler than ever to GetStarted™' next to the brown surface, 'Comprehensive tools for nanomechanics' next to the grid, and 'Widest range of accessories for materials science and bioscience' next to the instrument.

Plasmonic-enhanced performance for polymer solar cells prepared with inverted structures

Chuan-Sheng Kao,¹ Fang-Chung Chen,^{2,3,a)} Ching-Wen Liao,⁴ Michael H. Huang,⁴ and Chain-Shu Hsu⁵

¹*Institute of Electro-Optical Engineering, National Chiao Tung University, Hsinchu 30010, Taiwan*

²*Department of Photonics, National Chiao Tung University, Hsinchu 30010, Taiwan*

³*Display Institute, National Chiao Tung University, Hsinchu 30010, Taiwan*

⁴*Department of Chemistry, National Tsing Hua University, Hsinchu 30013, Taiwan*

⁵*Department of Applied Chemistry, National Chiao Tung University, Hsinchu 30010, Taiwan*

(Received 21 September 2012; accepted 25 October 2012; published online 9 November 2012)

We incorporated gold nanoparticles (Au NPs) in inverted organic photovoltaic devices to enhance the device performance. The photocurrent and fill factors were improved after the addition of Au NPs into the Cs_2CO_3 buffer layer. The photoluminescent measurements revealed a significant increase of light absorption of the photoactive layer. We attribute the improvement to local field enhancement induced by the localized surface plasmon resonance. Further, through the study of the morphologies of the cathode interfaces, we found that the rough surfaces might increase the device resistances. This drawback, however, was overwhelmed by the advantageous plasmonic effects. © 2012 American Institute of Physics. [<http://dx.doi.org/10.1063/1.4766736>]

Organic photovoltaic devices (OPVs) have been considered as one of the most promising systems for harnessing solar energy because of their light weight, mechanical flexibility, and the ability to prepare large-area panels at low cost.^{1,2} At present, OPVs based on the concept of bulk-heterogeneous junction can exhibit power conversion efficiencies (PCE) as high as 10%.³ The external quantum efficiency of OPVs is governed by its internal quantum efficiency and absorption efficiency.^{4,5} Because the former, which is affected by the diffusion and dissociation of excitons and charge collection, can now approaches almost 100%,⁵ the absorption efficiency remains one of the major problems toward even higher efficiencies.⁶ One feasible approach for increasing the absorption efficiency is to use a thicker photoactive layer. Nevertheless, due to the low carrier mobilities of organic materials, the use of too thick films inevitably increases the possibility of charge recombination and device resistance, thereby decreasing the charge collection efficiency.⁶⁻⁸ As a result, the challenge remains to achieve OPVs with high absorption efficiencies without degrading their internal quantum efficiencies.

Light trapping based on surface plasmon resonance (SPR) effects has attracted much attention as a means of improving the efficiency of OPVs.⁷⁻¹⁵ Various nanostructures, such as metallic nanoparticles, have been introduced into the devices for triggering SPRs.⁷⁻¹⁵ Their unique optical properties, including local field enhancement and strong light scattering, might improve absorption processes in OPVs. As for the device structures, most plasmonic-enhanced OPVs reported to date have been conventional ones. Because inverted device architectures eliminated the use of low-work-function metals, which are air-sensitive, they usually exhibited prolonged device lifetimes.¹⁶⁻¹⁸ Plasmonic-enhanced OPVs possessing an inverted structure, however,

are still very rare. In this work, we incorporated gold nanoparticles (Au NPs) into inverted OPVs to increase the light absorption efficiency. The Au NPs induced localized surface plasmon resonance (LSPR), which enhanced the local electromagnetic field of the active layer, thereby improving the device performance.

The devices were fabricated on indium tin oxide (ITO)-coated substrates. The device structure in this study is illustrated in Fig. 1(a). The ITO glasses were treated with UV-ozone prior to use. The Au NP solution was prepared

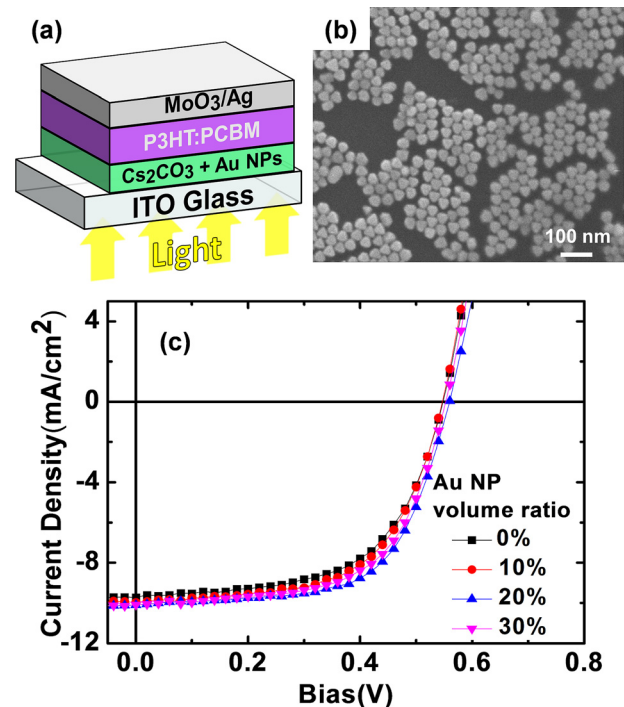


FIG. 1. Device structures of the OPVs in this study. (b) SEM image of the Au NPs. (c) J - V characteristics, recorded under illumination at 100 mW cm^{-2} (AM 1.5G), of the OPVs prepared with Cs_2CO_3 layers incorporating various amounts of Au NPs.

^{a)} Author to whom correspondence should be addressed. Electronic mail: fcchen@mail.nctu.edu.tw.

using procedures described previously.¹⁹ Fig. 1(b) displays the scanning electron microscopy (SEM) image of the Au NPs. The average particle size was ca. 45 nm. To prepare the cathodic buffer layer, the NP solution was blended into the Cs₂CO₃ solution with various volume ratios. Then, the composite solution was spin-coated onto the substrates, and the resulting thin film was annealed at 140 °C for 15 min. The photoactive layer comprised regioregular poly(3-hexylthiophene) (P3HT) and 1-(3-methoxycarbonyl)propyl-1-phenyl[6,6]methanofullerene (PCBM) at a weight ratio of 1:1. The photoactive film was spin-coated from a solution of 1,2-dichlorobenzene on the Cs₂CO₃ layer. After solvent annealing,^{20,21} the dried film was further annealed at 110 °C for 15 min. The thickness of the active layer was ~180 nm. Finally, a bilayer anode comprising MoO₃ (5 nm) and Ag (100 nm) was deposited through thermal evaporation. For the device characteristics, the photocurrent density-voltage (J - V) curves under illumination were measured using a Keithley 2400 source measure unit. The light source was a 150 W Thermal Oriel solar simulator. The IPCE measurements system (Enli Technology) comprised a quartz-tungsten-halogen lamp, a monochromator, an optical chopper, a lock-in amplifier, and a calibrated silicon-based diode.

Figure 1(c) displays the J - V characteristics of the OPVs prepared with various amounts of Au NPs. The device prepared with pristine Cs₂CO₃ exhibited an open-circuit voltage (V_{oc}) of 0.55 V, a short-circuit current (J_{sc}) of 9.73 mA cm⁻², and a fill factor (FF) of 0.58, resulting in a PCE of 3.12%. After the addition of Au NPs to the Cs₂CO₃ layer, the values of V_{oc} remained unchanged (0.55 V), suggesting that the cathodic interface was not affected too much by the Au NPs. Some portion of the surface of the NPs was probably also modified by Cs₂CO₃. The photocurrent and FF s, however, were improved (Table I). For the devices prepared with 20% Au NP solution, the J_{sc} and FF values were 10.11 mA cm⁻² and 0.64, respectively. As a result, the PCE was increased to 3.54%. Nevertheless, a further increase in the amount of the Au NP in the Cs₂CO₃ layer resulted in a decrease in the value of J_{sc} , presumably due to enhanced backward scattering and/or increased resistivity of the buffer layer. Notably, the values of the device series resistance (R_s), extracted from the J - V curves in the dark, indeed increased with the increasing Au NP concentrations. The results of extraction of R_s , listed in Table I, reveal that the enhanced device performance did not result from a reduction in device resistance.

Figure 2 displays the incident photon-to-electron conversion efficiency (IPCE) curves for various devices. Clearly, the

TABLE I. Electrical characteristics of devices incorporating various concentrations of Au NP solutions.

Concentration of Au NPs	V_{oc} (V)	J_{sc} (mA/cm ²)	FF	PCE (%)	R_s^a (Ω·cm ²)
0%	0.55	9.73	0.58	3.12	1.45
10%	0.55	9.97	0.59	3.23	1.40
20%	0.55	10.11	0.64	3.54	2.17
30%	0.55	10.09	0.61	3.38	2.81

^aDevice series resistance (R_s) was obtained from the inverse slope of the dark J - V curve.

photocurrent was increased after incorporating the Au NPs. One can also see that the trends in the IPCE follow those for the values of J_{sc} . We further compared the curve of the increase in IPCE (Δ IPCE) after the addition of 20% Au NPs with the extinction spectrum of the NPs (Fig. 2(b)). The wavelength regime, in which the IPCE values were increased, coincides with the extinction range of Au NPs, suggesting that excitation of LSPR indeed improved the efficiencies. Note that the extinction spectrum of the dilute Au NPs was relatively narrow. The real resonance peak of NPs should strongly depend on their surrounding media.^{7,22,23}

To understand the reason for the increased value of R_s of the device prepared with a higher concentration of Au NPs, we used atomic force microscopy (AFM) to observe the surface morphologies of the Cs₂CO₃ layers. Fig. 3 displays the AFM images of the buffer layers containing various amounts of Au NPs. We observed significant morphological changes on the surfaces after embedding the Au NPs. Further, the root-mean-square (rms) roughness of the surface prepared without Au NPs was 2.29 nm; the roughness increased with the concentration of Au NP solutions. They were 4.30 nm, 4.78 nm, and 5.23 nm for the samples fabricated with 10%, 20%, and 30% of NP solutions. These results suggest that the rough surfaces might induce trap states at the contacts and increase the device resistances. Fortunately, this drawback was overwhelmed by the advantageous plasmonic effects, thereby improving the overall device PCEs.

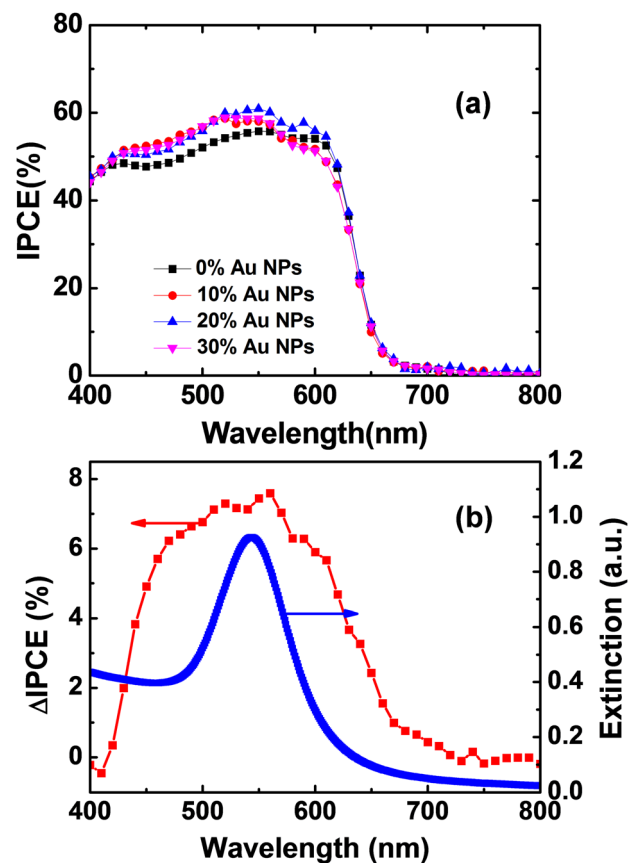


FIG. 2. IPCE spectra of the devices prepared with various concentrations of Au NP solutions. (b) Comparison between the curves of the increase in IPCE (Δ IPCE) after incorporating Au NPs and the extinction spectrum of the Au NPs suspended in water.

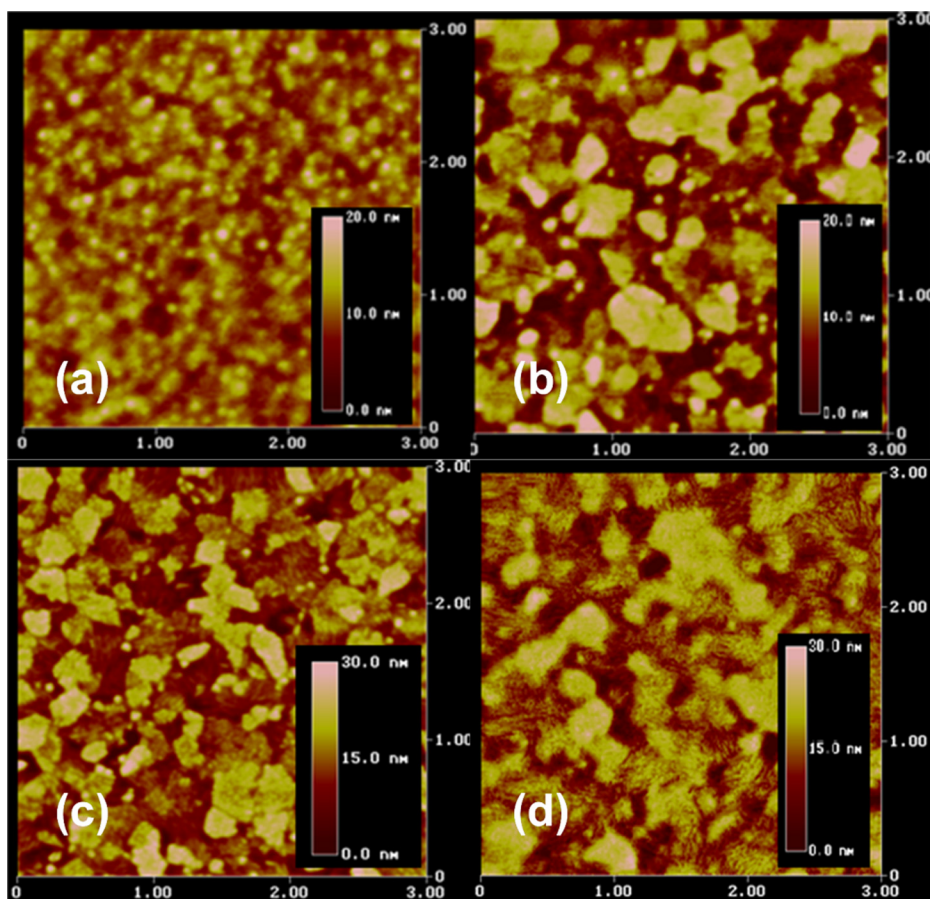


FIG. 3. AFM images ($3 \times 3 \mu\text{m}^2$) of the Cs_2CO_3 buffer layers prepared with various concentrations of Au NP solutions: (a) 0%; (b) 10%; (c) 20%; and (d) 30% Au NP solution doping.

Further, we performed the steady state photoluminescence (PL) measurements of the P3HT:PCBM thin films prepared on various Cs_2CO_3 buffer layers. The peak fluorescence intensity of the plasmonic sample was apparently enhanced by ca. 38% (Fig. 4). Because the resonance peak of the Au NPs was close to the absorption band of P3HT, we inferred that the enhanced PL was probably due to the increased level of photon absorption. Local enhancement of the electromagnetic field surrounding the Au NPs helped the energy dissipation, thereby increasing the total number of excitons in the photoactive layer.⁸

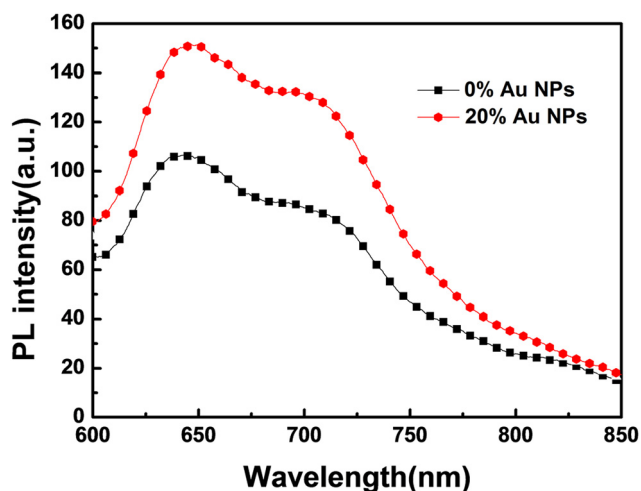


FIG. 4. PL spectra of the P3HT:PCBM thin films prepared with and without Au NPs. A 532-nm laser was used as the excitation source.

Previously, we blended Au NPs into the poly(3,4-ethylenedioxythiophene):polystyrenesulfonate (PEDOT:PSS) buffer layer to improve the device efficiencies.^{7,8} We attributed the improvement in device performance to the plasmonic effects. Another possible factor responsible for the increased photocurrent was related to the increased conductivity of the PEDOT:PSS layer after the addition of Au NPs.²⁴ The trace surfactants left behind the synthesis process of the Au NP solutions could change the morphology of PEDOT:PSS and increase its conductivity.²⁴ Nevertheless, this approach presented herein for constructing plasmonic-enhanced OPVs did not involve in the use of PEDOT:PSS. From the calculated series resistances, the cathode contacts were even deteriorated after the addition of Au NPs (Table I). Therefore, the results of this study can exclude the influence of the PEDOT:PSS layer and further confirm the plasmonic-enhanced mechanism of the Au NPs on the device performance.

In summary, we have improved the efficiency of inverted OPVs by incorporating Au NPs into the cathode buffer layer. The results of PL measurements revealed a significant increase of light absorption of the photoactive layer. The primary origin of the device improvement was local field enhancement induced by the LSPR. Through the study of the morphologies of the cathode interfaces, we found that the rough surfaces might increase the device resistances. Fortunately, this drawback was overwhelmed by the advantageous plasmonic effects. Because inverted devices usually exhibit longer device lifetime, we foresee that the results reported herein might be of further use in other material systems, such as low-band-gap polymers, to achieve even higher PCEs and enhanced stability.

We thank the National Science Council of Taiwan (Grant Nos. NSC 101-3113-E-009-005 and NSC 101-2628-E-009-008-MY3) and the Ministry of Education of Taiwan (through the ATU program) for financial support.

- ¹J. D. Servaites, M. A. Ratner, and T. J. Marks, *Energy Environ. Sci.* **4**, 4410 (2011).
- ²H. L. Yip and A. K. Y. Jen, *Energy Environ. Sci.* **5**, 5994 (2012).
- ³G. Li, R. Zhu, and Y. Yang, *Nat. Photonics* **6**, 153 (2012).
- ⁴J. Jo, S. I. Na, S. S. Kim, T. W. Lee, Y. Chung, S. J. Kang, D. Vak, and D. Y. Kim, *Adv. Funct. Mater.* **19**, 2398 (2009).
- ⁵S. H. Park, A. Roy, S. Beaupre, S. Cho, N. Coates, J. S. Moon, D. Moses, M. Leclerc, K. Lee, and A. J. Heeger, *Nat. Photonics* **3**, 297 (2009).
- ⁶D. H. Ko, J. R. Tumbleston, A. Gadisa, M. Aryal, Y. Liu, R. Lopez, and E. T. Samulski, *J. Mater. Chem.* **21**, 16293 (2011).
- ⁷F. C. Chen, J. L. Wu, C. L. Lee, Y. Hong, C. H. Kuo, and M. H. Huang, *Appl. Phys. Lett.* **95**, 013305 (2009).
- ⁸J. L. Wu, F. C. Chen, Y. S. Hsiao, F. C. Chien, P. Chen, C. H. Kuo, M. H. Huang, and C. S. Hsu, *ACS Nano* **5**, 959 (2011).
- ⁹K. Y. Yang, K. C. Choi, and C. W. Ahn, *Appl. Phys. Lett.* **94**, 173301 (2009).
- ¹⁰J. H. Lee, J. H. Park, J. S. Kim, D. Y. Lee, and K. Cho, *Org. Electron.* **10**, 416 (2009).
- ¹¹M. G. Kang, T. Xu, H. J. Park, X. Luo, and L. J. Guo, *Adv. Mater.* **22**, 4378 (2010).
- ¹²A. P. Kulkarni, K. M. Noone, K. Munechika, S. R. Guyer, and D. S. Ginger, *Nano Lett.* **10**, 1501 (2010).
- ¹³M. Xue, L. Li, B. J. Tremolet de Villers, H. Shen, J. Zhu, Z. Yu, A. Z. Stieg, Q. Pei, B. J. Schwartz, and K. L. Wang, *Appl. Phys. Lett.* **98**, 253302 (2011).
- ¹⁴W. E. I. Sha, W. C. H. Choy, Y. G. Liu, and W. C. Chew, *Appl. Phys. Lett.* **99**, 113304 (2011).
- ¹⁵J. Yang, J. You, C. C. Chen, W. C. Hsu, H. R. Tan, X. W. Zhang, Z. Hong, and Y. Yang, *ACS Nano* **5**, 6210 (2011).
- ¹⁶F. C. Chen, J. L. Wu, C. L. Lee, W. C. Huang, H. M. P. Chen, and W. C. Chen, *IEEE Electron Device Lett.* **30**, 727 (2009).
- ¹⁷S. K. Hau, H. L. Yip, N. S. Baek, J. Y. Zou, K. O'Malley, and A. K. Y. Jen, *Appl. Phys. Lett.* **92**, 253301 (2008).
- ¹⁸H. H. Liao, L. M. Chen, Z. Xu, G. Li, and Y. Yang, *Appl. Phys. Lett.* **92**, 173303 (2008).
- ¹⁹C. C. Chang, H. L. Wu, C. H. Kuo, and M. H. Huang, *Chem. Mater.* **20**, 7570 (2008).
- ²⁰G. Li, Y. Yao, H. Yang, V. Shrotriya, G. Yang, and Y. Yang, *Adv. Funct. Mater.* **17**, 1636 (2007).
- ²¹F. C. Chen, C. J. Ko, J. L. Wu, and W. C. Chen, *Sol. Energy Mater. Sol. Cells* **94**, 2426 (2010).
- ²²E. Hutter and J. H. Fendler, *Adv. Mater.* **16**, 1685 (2004).
- ²³K. L. Kelly, E. Coronado, L. L. Zhao, and G. C. Schatz, *J. Phys. Chem. B* **107**, 668 (2003).
- ²⁴D. D. S. Fung, L. Qiao, W. C. H. Choy, C. Wang, W. E. I. Sha, F. Xie, and S. He, *J. Mater. Chem.* **21**, 16349 (2011).